

Property evolution of thermo-mechanically treated reinforcement bar

V Musonda^{1,2a*}, ET Akinlabi¹ and TC Jen¹

¹Department of Mechanical Engineering Science, University of Johannesburg, Auckland Park Kingsway Campus, P.O. Box 524, Johannesburg, South Africa, 2006.

²Department of Mechanical Engineering, School of Engineering, The University of Zambia, Great East Road Campus, P.O. Box 32379, Lusaka, Zambia.

E-mail: ^{a*}musondachandi@gmail.com

Abstract. Property evolution of microstructure of reinforcement bar (rebar) depends on how well the steel is treated during and after the thermomechanical treatment (TMT) box. Rebars are hot rolled - from low carbon steel through Tempcore technology. In order to achieve optimal properties, typical evolving mechanical properties of the rebar such as ultimate tensile strength (UTS), yield stress (YS) and the percentage elongation (%El) were conducted. This is necessary to control the tempering and cooling process. In this study, a simulation of the cooling rebar was investigated using finite element modelling (FEM). The material used for the model and production of the rebar was equivalent to AISI 1016 carbon steel and was produced from scrap supplemented with direct reduced iron (DRI). The raw materials were melted in an electric arc furnace (EAF) prior to hot rolling through a billet caster. The rod mill tensile test report showed that UTS and YS values ranged between 482 MPa for the YS and 650 MPa for UTS on an average. The average percentage elongation was found to be 23 % well above the 14 % threshold according to the standard. The pearlite-ferrite microstructure and the martensite developed is in agreement with the standard microstructure found in the literature.

1. Introduction

Thermomechanical treated rebar is an appropriate material for reinforcing concrete structures because, the material's thermal expansion is similar to concrete structures [1]. Moreover, the material is compatible when it is bonded with concrete. The rebar has also the capacity to bear the maximum tensile stress acting on the structure [1, 2]. Apart from being key products to the construction industry, concrete rebars are also high quality materials which can meet the consumers' concerns about the standard mechanical properties for their applications [3]. TMT rebars are often used in constructing bridges, and are also useful in the general fabrication works, where bending, machining and welding is required. To obtain the optimal properties of the rebars, the hot rolling process should have an authentic Tempcore technology [4, 5]. Steel billets are used in the hot rolling of rebars and the latter is subjected to an on-line TMT in three consecutive phases namely, quenching, self-tempering and atmospheric cooling respectively [4].

In the first phase, hot-rolled rebar leaving the final finishing stand at approximately 850°C and at a speed of 11.5 m/s, is quickly quenched in the TMT chamber by a water spray system. The surface of the rebar is consequently hardened to a depth optimized for each profile and this results in the creation of martensite rim. At this stage, however, the core is still hot and austenitic. In the self-tempering stage the core of the rebar is still hotter than the surface. Therefore, the difference in temperature between



the core and the surface allows the heat to flow from the core to the surface and this is what causes the martensite to be “tempered martensite” [1, 2, 4, 5, 6, 7]. The final phase is the cooling bed where there is free cooling of the rebars. This is where the transformation of austenitic core begins to change into ductile pearlite-ferrite structure. Finally an optimum mixture of hard tempered martensite rim with a ductile core of ferrite and pearlite at the centre is formed [5]. Depending on the values of the controlling parameters, there can be a transition zone (TZ), where the layer typical of austenite below the quenched surface can transform completely or partially to bainite.

Recently two Tempcore models have been developed [8, 9]. The first model calculates the time required to quench the material in order to obtain the minimum yield strength, yield stress (YS) and other rebar data such as, diameter and finishing temperature. The internal diameter of cooling nozzles in the TMT box and the specific water flow rate can then be selected and an equation for the calculation of quenching time can be derived as in equation (1) [9]:

$$\tau = K_1 \cdot \frac{\phi^a \cdot T_0^b YS^c}{q^d \cdot F^e} \quad (1)$$

There is need to establish the relationship between the mechanical properties and the chemical composition of the rebar. Hence in the second model [9], the appropriate equation which defines this relationship is as shown in equation (2).

$$TS = K_2 \cdot C^\alpha \cdot Mn^\beta \cdot YS^\gamma \cdot \phi^\delta \quad (2)$$

In equation (1) and (2):

τ is the time for quenching (s), ϕ is diameter of rebar (mm), T_0 is the temperature at entry ($^{\circ}\text{C}$), YS is yield strength (MPa), TS is tensile strength (MPa), q is linear water flow rate (m^3/h per m of line), F is the coefficient of filling, where $F = \phi^2/\text{ID}^2$ and ID is the internal diameter of the cooling nozzle, C is the wt.% of carbon in steel, Mn is wt.% of manganese in steel and ($K_1, K_2, a, b, c, d, e, \alpha, \beta, \gamma, \delta$) are constants. Using the two equations (1) and (2), five other relationships can be established where the quenching time (τ) is taken as a dependent variable being the function of other independent variables such as $\tau = f(\text{ID}, q)$ [9]. However, the typical criteria for optimisation of a Tempcore installation is to consider (i) total cooling water flow rate and pressure, (ii) overall length of the equipment and (iii) number of sets of cooling nozzles. Other requirements in optimising the quenching process in the TMT box, are that, the Tempcore installation should also consider the constraints in the mill, the straightness of the rebar, and how the process can be controlled [8,9].

2. Modelling and Heat transfer during cooling

2.1. Material model

Residue stresses can develop during the deformation of the workpiece in a metal forming process such as rolling. This is due to the variations in the distribution of temperatures in the material. In the same manner, temperature distributions in the workpiece can also vary while quenching and cooling the workpiece and this can also lead to the formation of residue stresses which consequently can affect the grain size and the strength of the material. In this study, DEFORM 3D FEM software was used in the simulation of heat transfer in the rebar in order to evaluate the temperature distribution. Arbitrary Lagrangian-Eulerian (ALE) formulation was used in the analysis [10]. A three-dimensional numerical model in DEFORM 3D was also conducted by Pashazadeh *et al.* [11] to investigate mechanical, thermal and material flow characteristics in friction stir welding (FSW) of copper sheets. The authors [11] used ALE formulation in their simulation. Only a quarter symmetry was modelled in this study.

2.2. Heat transfer during quenching

2.2.1. Heat conduction in a solid

Whenever there is transfer of heat from higher temperature to lower temperature, localized temperature gradients develop in the workpiece [12]. The Fourier's law of heat transfer Q , can then be used to describe the relationship between the temperature gradients with the given heat transfer rate, where the transfer rate of heat per unit area is considered to be proportional to the local temperature gradient. This law can be expressed as in equation (3)

$$Q = -\lambda A \frac{\delta T}{\delta x} \quad (3)$$

In equation (3), Q is the transfer rate of heat in J/s, λ is the thermal conductivity in J/(s m K), A is the unit area in m^2 , T is the temperature in K, and x is a local coordinate. If there are no heat sources in a solid and the temperature within the solid changes with time, then the heat transfer in this case can be expressed as in equation(4) [12].

$$\frac{\partial T}{\partial t} = a \left(\frac{\delta^2 T}{\delta x^2} + \frac{\delta^2 T}{\delta y^2} + \frac{\delta^2 T}{\delta z^2} \right) \quad (4)$$

In equation (4), t is the time in seconds(s), a is the thermal diffusivity in m^2/s , while x , y , and z are local coordinates. The thermal diffusivity a is defined as in equation (5)

$$a = \frac{\lambda}{\rho C_p} \quad (5)$$

In equation (5) ρ is the density in kg/m^3 and C_p is the specific heat capacity under constant pressure in J/ (kg K).

2.2.2. Material input parameters and procedures

The composition of the material in this study is defined as follows: 0.23% C, 0.3% Si, 0.6% Mn, 0.025% P, 0.034% S, 0.23% Cr, 0.30% Cu and Fe balance. This was obtained using an Optical Emission Spectrometer (OES). The workpiece was modelled as rigid –plastic material, with 4212 mesh elements and 5143 nodes. Tensile tests and bend tests on twenty four (24) Y16 mm rebar samples were conducted using a computerised TUE-C-600 Universal Testing Machine. The bending test was conducted according to ASTM E-290 standard [13]. Metallographic specimen preparation was conducted according to ASTM E3-11[14].

3. Results and discussion

3.1. Temperature distribution profile

The temperature distribution in the modelled workpiece is shown in figure 1(a) to (d). There is a temperature drop of 19°C in 4.5 seconds during the initial cooling (figure 1(a)). In the middle of the cooling process at step 70 in figure 1(d) the temperature dropped to 818°C minimum in 10.5 seconds and 840°C maximum. The maximum temperature at the end of cooling process was 831°C after 15 seconds (step100 not in the report). Heat flow in solids is also usually considered as a diffusion-like process. In this case the temperature distribution is regarded as a system of the equation of linear flow of heat. The linearity is, however, very pronounced in the heat flux graphs in figure 2.

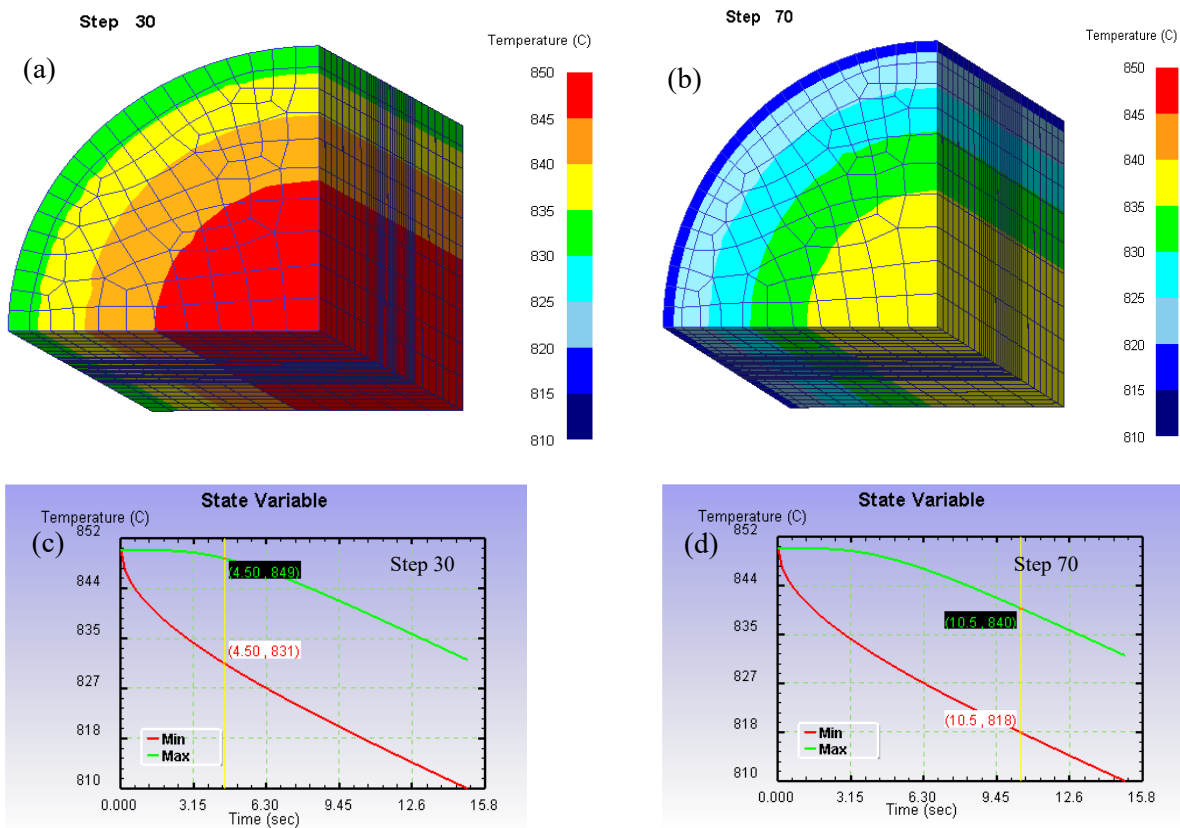


Figure 1. (a) Temperature contours at step 30 (b) Temperature contours at step 70(c) Temperature profile at step 30, (d) Temperature profile at step 70.

3.2. Heat rate and heat flux

The change in temperature from 850°C to 840°C due to the heat flow, is demonstrated in figure 2 (a) and (b). It can be seen that the heat is propagating in the negative direction and drops to -4.96×10^5 N-mm/sec before rising to -4.7×10^5 N-mm/sec initially and then rises to a maximum of -4.52×10^5 N-mm/sec in a linear fashion in figure 2(b) step 70. It should be noted that, the maximum temperature reached after cooling is 831°C in 15 seconds, signifying a drop of approximately 20°C. Despite this drop, the core is still hot at this temperature and austenitic.

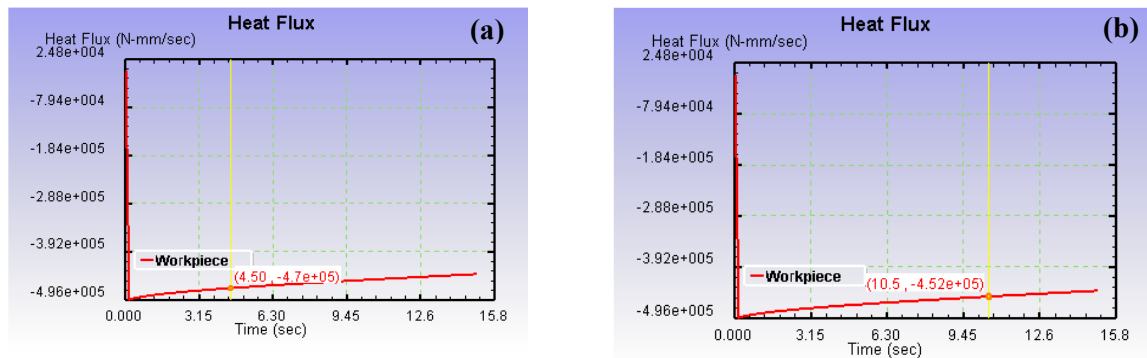


Figure 2. (a) Heat flux profiles at step 30, (b) Heat flux profiles at step 70.

3.3. Microstructural Investigation

The optical micrographs of the martensite rim at the periphery and the pearlite-ferrite microstructure at the core respectively are shown in figure 3 (a) and (b). The micrographs depicts complete recrystallization after hot rolling with finer grains at the core dominated by ferrite (light areas). Figure 3(c) shows secondary electron image (SEI) on a selected sample taken using VEGA 3 TESCAN Oxford Instruments X-Max 50 mm² scanning electron microscope (SEM). Spectrum 5 (figure 3(d)), the energy dispersive spectroscopy (EDS), shows the elemental composition of the material. It can also be observed that there is consistency in the amount of manganese detected by OES and EDS despite some variations in certain elements. The quantities are within permissible limits of (wt. % 0.6). Manganese is basically a deoxidizer and a desulfurizer which is present in almost all steels [12, 15]. The tendency for macro segregation is less compared to other common elements. 0.60% Mn is apparently recommended in rebars, and it becomes impossible to rim steels above this limit. Manganese is beneficial as it promotes surface quality in most carbon steels. It also affects weldability and forgeability favourably.

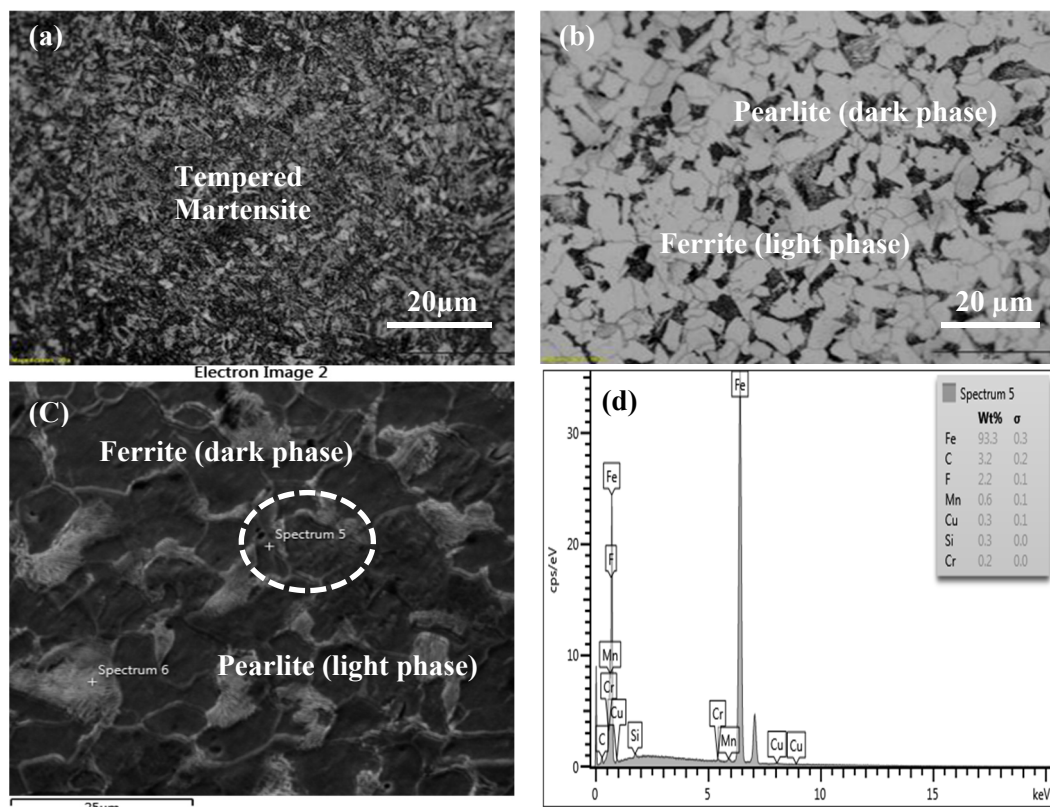


Figure 3. Micrographs for Y16 rebar: (a) Tempered Martensite(TM) (b) Transverse section of ferrite(light phase) and pearlite (dark phase) all taken at 20 μm (c) SEM Polygonal ferrite(PF) dark phase, and pearlite (light phase) at 20 KV, (d) EDS-chemical composition of Y16 mm rebar for spectrum 5.

4. Conclusion

Metallurgical transformations of kinetics and the flow stress behavior of the material are controlled by the temperature which seemingly is the main parameter. With proper control of parameters in TMT box such as dwell time during quenching, water flow rate and the speed of the mill, the final structure and appropriate inherent properties of the rebars can be achieved. The dwell time for quenching depends on the diameter of the rebar. The range, however, is between 0.5 to 0.8 seconds for a Y12 or

Y16 rebar. The key, nevertheless, is to quench the rebar in less than one second ($< 1\text{sec.}$), at controlled water flow rate so that carbon content is controlled. In this study, property evolution of TMT rebar to establish the microstructure and the required mechanical properties has been achieved by the prediction of the expected temperature profiles and other mechanical tests. The results obtained are in agreement with existing literature.

Acknowledgements

We wish to thank the management and workshop staff of Kafue Steel Plant at Universal Mining and Chemical Industries Limited in Zambia for allowing us to tour their plant and see the actual production of steel.

References

- [1] Souvik D, Mathur JT, Bhattacharyya S and Bhattacharyya, 2014 Failure analysis of rebars during bending operations, *Case Studies in Engineering Failure Analysis* **2** 51–53.
- [2] Chakrabarti I, Bhattacharyya T, Maheshwari MD, Venugopalan T, and Chakravorty AK 2006 High strength rebars for the Indian construction industry. *Tata Search* **2**:395–403.
- [3] Musonda V, Akinlabi ET and Jen TC 2017 Effect of Water flow Rate on the Yield Strength of a Reinforced bar, *Advances in Engineering Research (AER)*, volume **102** 353 *2nd Int. Conf.on Mechanics, Materials and Structural Engineering (ICMMSE)*, January, DOI:10.2991/icmmse-17,58, Atlantis Press.
- [4] BAŁA P 2009 Tempcore process analysis based on the kinetics of phase transformations, *Archives of Metallurgy and Materials*, Volume **4**, issue 4. Available online, http://imim.pl/files/archiwum/Vol4_2009/42.pdf, accessed on 21 April 2018.
- [5] Markan RK 2005 Steel reinforcement for India, relevance of quenching & tempering technology. *Steel World*; p. 4 – 9.
- [6] Madias Wright M, and Wolkowicz P 2017 Reinforcing Bar: Hardening Mechanisms and Performance in Use, *Conference: AISTech 2016 proc.*, pp. 2287-2296.
- [7] Kabir IR, and Islam MA 2014 Hardened Case Properties and Tensile Behaviours of TMT Steel Bars, *American J. Mech. Eng.* **2**(1) 8-14'
- [8] Simon P, Economopoulos M, and Nilles P 1984 Tempcore, an economical process for the production of high quality rebars; *MPT*, No. **3**, P. 80-93.
- [9] Simon P 1990 Optimization of Tempcore installations for rebars; *MPT*, No. **2**, P. 61-69
TEMPCORE® is a registered trademark of Centre for Research in Metallurgy (CRM).
- [10] DEFORM http://www.artech-eng.ru/images/stories/Stat/DEFORM/Readme_DEFORM_v10.2.pdf
- [11] Pashazadeh H A Masoumi A and Teimournezhad J 2013 *Int. J. of Automotive Engineering* Vol. **3**, Number 1, March.
- [12] Totten GE 2006 *Steel heat treatment: Metallurgy and technologies*, CRC Press.
- [13] ASTM E 290-97A, 2006. "Standard Test Methods for Bend Testing of Material for Ductility", ASTM International, PA, USA. (www.astm.org).
- [14] ASTM E3-11 2011 Standard guide for preparation of metallographic specimens.
- [15] Ross RB 1992 *Metallic Materials Specification Handbook*, 4th ed., Chapman & Hall, London.